American Mineralogist, Volume 73, pages 232–241, 1988

Subsolidus phase equilibria on the forsterite-saturated join $Mg_2Si_2O_6$-$CaMgSi_2O_6$ at atmospheric pressure

WILLIAM D. CARLSON
Department of Geological Sciences, University of Texas at Austin, Austin, Texas 78713, U.S.A.

ABSTRACT

The marked discrepancies among recent studies of pyroxene phase equilibria in the system CaO-MgO-SiO_2 at atmospheric pressure can be largely resolved by data generated in experiments using V_2O_5 and PbO as solvents at temperatures from 925 to 1425 °C. These experiments confirm the existence, on the 1-atm isobar, of stability fields for solid solutions of diopside, pigeonite, protoenstatite, orthoenstatite, and an orthopyroxene-like phase stable only at temperatures between 1370 and 1445 °C. Compositional reversals define within narrow limits the extent of miscibility between coexisting phases over the range 925–1370 °C, and synthesis results from 1370 to 1425 °C are demonstrably in agreement with all data from other sources for which the attainment of equilibrium can be inferred with confidence.

Three isobarically invariant equilibria are stable at atmospheric pressure. The reaction of orthoenstatite to protoenstatite + diopside is reversed using a plumbate solvent at 1005 ± 10 °C, replicating earlier results obtained with vanadate solvents. The reaction of protoenstatite + diopside to pigeonite is reversed using vanadate solvents at 1295 ± 10 °C. The reaction of protoenstatite + pigeonite to an orthopyroxene-like phase is constrained by synthesis results to occur at 1370 ± 10 °C, but this reaction could be driven to completion only in the up-temperature direction.

In addition to the mineralogical implications of precise thermal and compositional limits for the polymorphism and mutual stabilities of various low-Ca pyroxenes, these results add new constraints to thermodynamic models fundamental to thermobarometry of natural pyroxene-bearing assemblages.

INTRODUCTION

Despite experimental efforts extending over three decades, subsolidus phase equilibria along the forsterite-saturated join $Mg_2Si_2O_6$-$CaMgSi_2O_6$ at atmospheric pressure have remained uncertainly known. Sluggish reaction kinetics and a confusing array of pyroxenes with closely similar physical properties make the determination of equilibrium phase relations at subsolidus temperatures a difficult and complicated task. Nevertheless, a definitive identification of the stable phase assemblages in this system and of the limits of mutual solid solution among phases is essential. Petrologically, these phase equilibria add valuable constraints to thermochemical models used for pyroxene thermometry and serve as a guide to theory and experiment in chemically more complex systems. Mineralogically, the phase equilibria illustrate the complexity of the polymorphism possible in some ranges of pyroxene composition and illuminate the importance of slight chemical variations in determining the stability of polymorphs capable of limited solid solution.

This report contributes a set of experimental data at subsolidus temperatures encompassing, for the first time, equilibria among all of the pyroxenes now known to occur in $Mg_2Si_2O_6$-$CaMgSi_2O_6$ at atmospheric pressure. The use of V_2O_5 and PbO as high-temperature solvents in the experiments (cf. Carlson, 1986a) has produced rapid attainment of chemical equilibrium and has promoted crystal growth to sizes permitting unambiguous phase identification and accurate chemical analysis by electron-microprobe techniques. These advantages have made it possible to generate data that resolve many of the mutual contradictions among previously published studies in this system.

PREVIOUS WORK

Early syntheses in the system $Mg_2Si_2O_6$-$CaMgSi_2O_6$ at atmospheric pressure by Atlas (1952), Boyd and Schairer (1964), Kushiro (1972), Yang and Foster (1972), and Yang (1973) produced agreement on the general features of the equilibria in the temperature range from ~900 to ~1400 °C. Diopside solid solution (Dio) coexists, across wide miscibility gaps, with a succession of low-Ca pyroxene solid solutions, first with orthoenstatite (Oen) at low temperatures, then with protoenstatite (Pen) at intermediate temperatures, and ultimately with pigeonite (Pig) at high temperatures up to the diopside-saturated solidus.

The discovery by Foster and Lin (1975) of a stability field for a Ca-poor orthorhombic phase near 1400 °C led

0003–004X/88/0304–0232$02.00

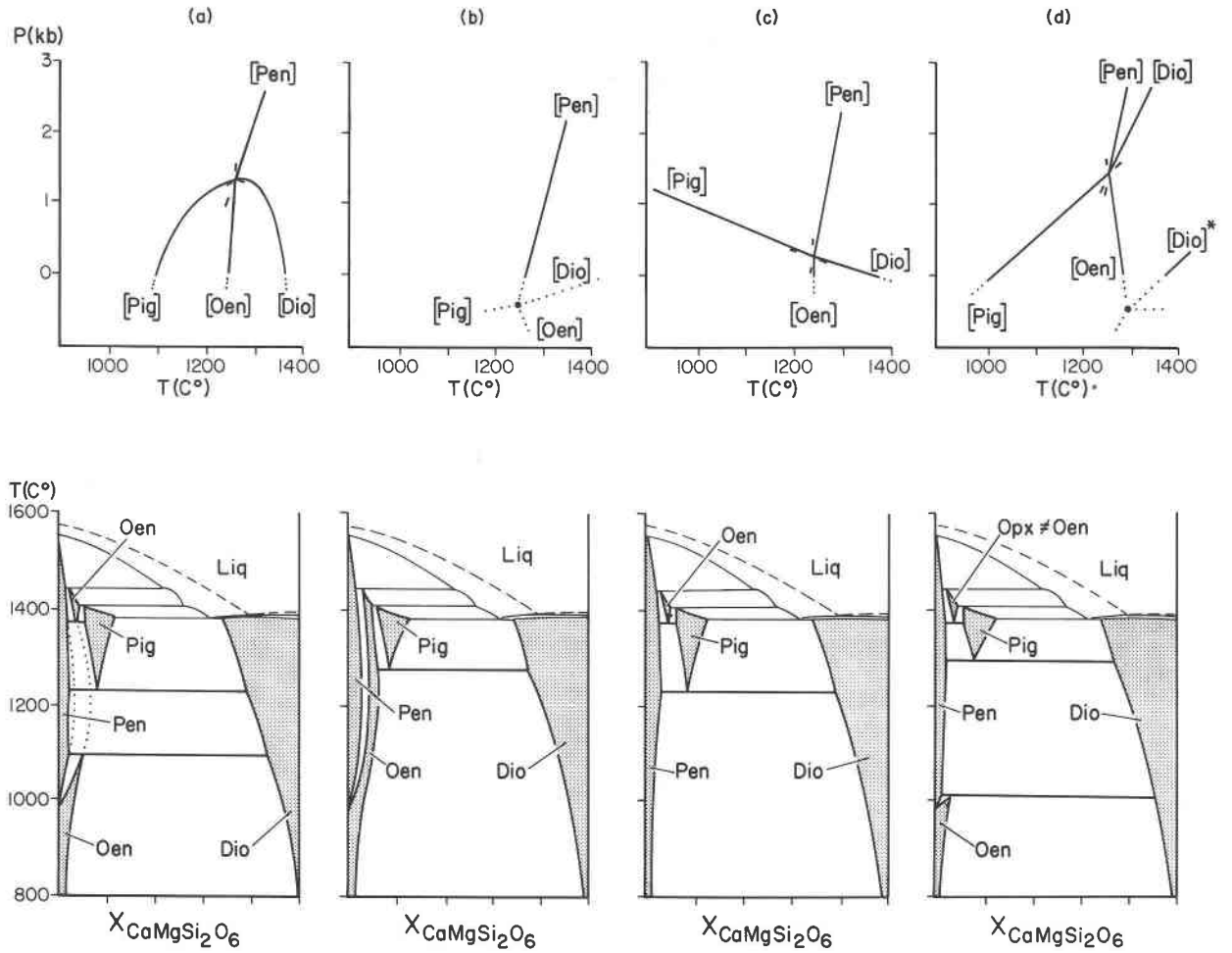

Fig. 1. Comparison of proposed versions of phase equilibria: (**a**) after Longhi and Boudreau (1980); (**b**) after Jenner and Green (1983); (**c**) after Biggar (1985); (**d**) after Carlson (1985, 1986b). In schematic *P-T* projections (top), dotted lines represent extrapolation of phase equilibria to pressures below the 1-atm isobar; at high temperatures, melting will truncate some of the equilibria shown. "[Dio]*" in (d) references the reaction Pen + Pig = Opx. In schematic 1-atm *T-X* sections (bottom), widths of stability fields are exaggerated for clarity; all supersolidus boundaries (light lines) are derived from Longhi and Boudreau (1980); dotted lines in (a) represent metastable extension of miscibility gap between Oen and Pen.

to a series of investigations (Longhi and Boudreau, 1980; Jenner and Green, 1983; Biggar, 1985; Carlson, 1985, 1986b) that yielded highly discrepant interpretations for equilibria in the Mg-rich portion of the system. All investigators have encountered, in runs quenched from temperatures in the range 1370 to 1445 °C, a phase with optical properties and X-ray powder-diffraction spectra indistinguishable from those of the orthoenstatite encountered below ~1000 °C at atmospheric pressure. Longhi and Boudreau, Jenner and Green, and Biggar have regarded the high-temperature orthorhombic phase as the precise equivalent of Oen, whereas Carlson has hypothesized that it might be a distinct polymorph. In the following discussion, this phase will be referred to simply as orthopyroxene (Opx), to permit clear distinction from Oen while acknowledging the possible equivalence of the two phases.

In previous work, the complications that are introduced by a stability field near 1400 °C for Opx have been resolved by four distinctly different interpretations. The essential features of each interpretation are illustrated in Figure 1, using schematic *P-T* projections of the binary univariant (three-pyroxene) equilibria and *T-X* sections through the equilibria at the 1-atm isobar. The univariant three-pyroxene equilibria of interest radiate from the invariant point at which Pen, Oen, Pig, and Dio are simultaneously stable. Although the position of this invariant point is an important feature in every interpretation, constraints on its location are few. Warner (1975) placed this invariant point with considerable uncertainty in the region 1240–1280 °C, 1–2 kbar; the thermodynamic model of Carlson and Lindsley (1988) places it near 1250 °C, 1.1 kbar. (Each equilibrium terminating at this invariant point is identified by enclosing in brackets the phase not

participating in reaction along that equilibrium; e.g., [Oen] references the reaction Pen + Dio = Pig.)

Longhi and Boudreau (1980) regarded Opx as equivalent to Oen, and by relying upon the subsolidus diagrams of Atlas (1952) and Boyd and Schairer (1964), they inferred a split stability field for Oen = Opx (Fig. 1a, bottom). Because, as Jenner and Green (1983, p. 154) pointed out, [Dio] must have a steeper dP/dT slope at the invariant point than [Pig], the interpretation of Longhi and Boudreau requires strong curvature along either [Dio] or [Pig] or both (as shown here in Fig. 1a, top), to produce an intersection of [Dio] with the 1-atm isobar. Such curvature along these solid-solid reactions would necessitate somewhat unusual thermodynamic properties for the low-Ca pyroxenes.

Jenner and Green (1983) also considered Opx equivalent to Oen, but rejected the evidence then available for intersections of [Pig] and [Oen] with the 1-atm isobar. They placed the invariant point below 1 atm and inferred that all Pen + Dio equilibria are metastable with respect to Pen + Oen and Oen + Dio equilibria (Fig. 1b).

Biggar (1985) accepted the evidence for [Oen] at 1 atm, but noted that the data of Atlas (1952) and of Boyd and Schairer (1964) on [Pig] were based upon hydrothermal experiments at H_2O pressures of 500–1000 bars and thus did not require [Pig] to occur on the 1-atm isobar. Explicitly in order to avoid imposing curvature upon the equilibria, he assigned a very low pressure to the invariant point and a shallow negative dP/dT slope to [Pig]. The distinguishing feature of this interpretation is that it does not generate an intersection of [Pig] with the 1-atm isobar, but it does permit [Dio] to appear at high temperatures without any curvature along it (Fig. 1c). Biggar deliberately did not continue his T-X section below 1250 °C. The extension to lower temperatures shown here (Fig. 1c, bottom) depicts the phase relations that arise as a necessary consequence of the P-T relations published in Biggar's Figure 11 (reproduced here in Fig. 1c, top).

Carlson's (1985) subsequent 1-atm reversal of [Pig] at 1005 ± 10 °C conflicts with Biggar's interpretation. As an alternative to the very marked curvature of [Dio] shown in the P-T projection of Figure 1a, Carlson proffered the hypothesis that Opx is a distinct phase from Oen, one which may have a similar structure and may even invert to Oen on quench. This interpretation (Fig. 1d) eliminates the necessity for strong curvature along [Dio] and/or [Pig] by introducing additional univariant equilibria emanating from an invariant point below 1-atm pressure, at which Pen + Opx + Pig + Dio are stable.

The resolution of these conflicting interpretations clearly requires careful identification of the univariant three-pyroxene assemblages stable on the 1-atm isobar. This study defines and locates three such assemblages, corresponding to the equilibria [Pig], [Oen], and either of the two possible [Dio] equilibria (Pen + Pig = Oen or Pen + Pig = Opx). The data are therefore consistent with the interpretations of either Longhi and Boudreau (1980) or Carlson (1985), but rule out the interpretations proposed by both Jenner and Green (1983, their Fig. 4) and Biggar (1985, his Fig. 11).

Experimental and analytical techniques

The experimental methods employed in this study are similar to those described in Carlson (1986a, 1986b), with differences as noted below. Vanadate solvents with the compositions given in Figure 2 were used in most experiments; a plumbate solvent was also used in a few runs to replicate earlier low-temperature results on the [Pig] reaction. The effects of these solvents on the inferred phase equilibria are considered to be negligible, as discussed in a separate section below. The marked changes in solubility of the pyroxene components (especially silica) at high temperatures made careful control of temperature and accurate knowledge of the saturation levels in the solvent essential. Table 1 describes the variety of crystalline, glass, and oxide starting materials that were mixed with the solvent in proportions ranging from 2:1 to 1:2 by weight, then loaded in 0.05-g aliquots into the bottom portions of 3-cm-long, 2.5-mm-diameter Pt capsules. Each capsule was squeezed flat over its whole length, dried for 48 h at 600 °C, then welded closed. The unfilled top portion of the capsule allowed for expansion on heating; in the absence of a confining pressure, this precaution was essential to prevent bursting of the capsule and consequent evaporation of the solvent in high-temperature runs. Run durations decreased from 5 d near 900 °C to 1 d near 1400 °C. Temperatures were measured with Pt-$Pt_{90}Rh_{10}$ thermocouples, calibrated to the melting of Au at 1064 °C and the liquidus of diopside at 1392°C, placed adjacent to capsules suspended in a vertical quench furnace; decalibration of thermocouples at high temperatures was eliminated by an arrangement that allowed their extraction and re-insertion, limiting their exposure to high temperatures to the duration of the measurement itself. Run temperatures fluctuated no more than ±2 °C and are believed accurate to approximately ± 5 °C on the basis of the reproducibility of melting-point calibrations.

After runs were quenched in water and dried at 110 °C, a chip was polished for reflected-light and microprobe analysis, and the remainder of the charge was leached of solvent in acid (cold 4% HCl for vanadates and hot 1:1 HNO_3 for plumbates), then boiled briefly in 0.5M NaOH to remove any residual silica-rich gel. The crystalline product thus extracted was examined in immersion liquids on a petrographic microscope, by scanning electron microscopy, and by X-ray powder diffraction.

All experiments reported here produced two or three pyroxenes in mutual equilibrium and coexisting with forsterite (For). Phase identifications were made with great certainty on the basis of petrographic, X-ray powder diffraction, and electron-microprobe data and agree in all cases with the reinterpretations and criteria for recognition advanced by Biggar (1985). Optical and X-ray observations were always sufficient to discriminate among Pen, Oen or Opx, Dio, and low-Ca clinopyroxene. Low-Ca clinopyroxene could be identified certainly either as Pig or as clinoenstatite (Cen) inverted from Pen only after electron-microprobe analysis. Following Biggar (1985), low-Ca clinopyroxenes are discriminated on the basis of their distinctly different Ca contents: Pig in these experiments always bears 3–6 wt% CaO, whereas Cen bears 1 wt% or less.

Electron-microprobe analysis was performed by wavelength-dispersive methods on a JEOL 733 instrument. Analytical standards were a synthetic glass containing CaO, MgO, Al_2O_3, FeO, and SiO_2 (NBS Standard Reference Material no. 470 = Glass K412) for Ca, Mg, and Si; synthetic crystalline V_2O_5 for V; and

a synthetic lead silicate glass (NBS Standard Reference Material no. 1871 = Glass K456) for Pb.

Experimental results and equilibrium criteria

Pyroxenes appear in run products as short, subhedral to euhedral prisms. Most grains are 10 to 100 μm in diameter, although Opx characteristically grows to much larger sizes, often an order of magnitude larger than coexisting phases. All pyroxenes show pale blue cathodoluminescence under the electron beam. Pig, Dio, and Opx are all faintly blue in powders, and although Pen in low-temperature runs is faintly yellow-green in transmitted light and in powders, it too takes on a more bluish tinge in higher-temperature runs. Pen invariably shows at least partial inversion on quench to Cen (Smith, 1959; Smyth, 1974; Longhi and Boudreau, 1980; Carlson, 1986b), as indicated by characteristic powder X-ray reflections and optically by the formation of polysynthetic twins on (100) with extinction angles of 23–25° and the development of fractures perpendicular to the prism length. This partially to wholly inverted material in run products (referenced here as Pen/Cen) is interpreted to have formed originally as Pen. Because of twinning and cracking on inversion, crystals of Pen/Cen are often cloudy and whitish, in contrast to the relative clarity of small Pig and Dio crystals and the gemlike transparency of large Opx crystals.

Crystallization during the 3 to 5 s required to quench the charges occurred only from the highly siliceous solvents present in runs at temperatures above ~1275 °C. In these runs, a corona of tiny elongate diopside prisms with coxcomb structure often formed around the much larger pyroxenes that represent the equilibrium assemblage. This distinctive texture, combined with the extremely high V contents of the quench crystals (1–2 wt% V_2O_4, compared to values typically less than 0.5 wt% for the equilibrium phases; see Table 2), made recognition of this quench phase straightforward.

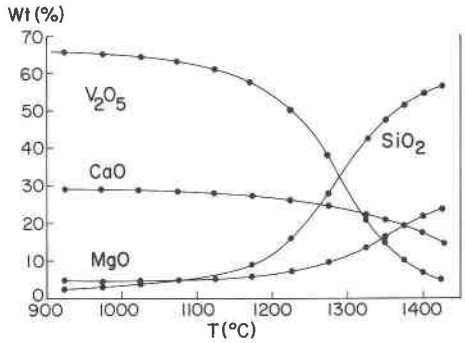

Fig. 2. Compositions of vanadate solvents saturated with Oen + Dio + For (T < 1005 °C), Pen + Dio + For (1005 °C < T < 1295 °C), Pen + Pig + For (1295 °C < T < 1370 °C), and Pen + Opx + For (T > 1370 °C). Solvents saturated with Pig + Dio + For (1295 °C < T < 1375 °C) and with Opx + Pig + For (1370 °C < T < 1400 °C) are slightly richer in CaO than their counterparts in the same temperature range plotted here; these differences were insignificant to the crystalline assemblage formed in experiments using weight ratios of solvent : reactant of 1:1 or less. Discontinuities in solvent compositions across univariant reactions are too small to be resolved by these experiments.

Table 2 contains data on the assemblages and pyroxene compositions in those experiments that produced two or more pyroxenes in mutual equilibrium. None of the analyzed pyroxenes displayed appreciable compositional zoning, and the standard errors of the compositional mean given in Table 2 document the small magnitude of variations in compositions present among crystals in a run. The phase diagram based upon the results in Table 2 is presented in Figure 3. At temperatures below 1175 °C,

TABLE 1. Reactants

Reactant	Mineralogical equivalent	Description
OXD1	Pen	2 MgO·2 SiO_2
OXD2	Dio	CaO·MgO·2 SiO_2
OXD3	For	2 MgO·SiO_2
OXD4	Pig	0.893 OXD1 + 0.107 OXD2
OXD5	Opx	0.923 OXD1 + 0.077 OXD2
OXD6	Pen + Opx + For	0.333 OXD1 + 0.333 OXD5 + 0.333 OXD3
OXD7	Opx + Pig + For	0.333 OXD5 + 0.333 OXD4 + 0.333 OXD3
GLS1	Pen + Dio + For	Glass prepared by fusing 0.333 OXD1 + 0.333 OXD2 + 0.333 OXD3 at ~1500 °C
GLS2	Opx + For	Glass prepared by fusing 0.667 OXD5 + 0.333 OXD3 at ~1600 °C
XTL1	Pen + Dio + For	GLS1 crystallized at 925 °C to yield Pen/Cen[0.016] + Dio[0.904] + For
XTL2	Pen + Dio + For	GLS1 crystallized at 1175 °C to yield Pen/Cen[0.028] + Dio[0.804] + For
XTL3	Pen + Dio + For	GLS1 crystallized at 1285 °C to yield Pen/Cen[0.037] + Dio[0.744] + For
XTL4	Pig + Dio + For	GLS1 crystallized at 1305 °C to yield Pig[0.166] + Dio[0.731] + For
XTL5	Pig + Dio + For	GLS1 crystallized at 1375 °C to yield Pig[0.222] + Dio[0.648] + For
XTL6	Pen + Pig + For	GLS2 crystallized at 1305 °C to yield Pen/Cen[0.035] + Pig[0.156] + For
XTL7	Pen + Pig + For	GLS2 crystallized at 1360 °C to yield Pen/Cen[0.033] + Pig[0.114] + For
XTL8	Opx + For	GLS2 crystallized at 1400 °C to yield Opx[0.070] + For
XTL9	Oen + Dio + For	GLS1 crystallized at 850 °C, 2000 bars H_2O, to yield a metastable mixture of Pen/Cen + Oen + Dio + For, too fine-grained for microprobe analysis

Note: Proportions in mixtures are mole fractions using six oxygens per formula unit for pyroxenes, four for forsterite. Bracketed values are mole fractions of $CaMgSi_2O_6$ in crystalline starting materials as determined by electron-microprobe analysis. Reactants XTL1 to XTL8 were crystallized in the presence of saturated V_2O_5-rich solvents, the compositions of which are given in Fig. 2.

TABLE 2. Summary of experimental results

T (°C)	Reactant*	Products†	n	Weight percent CaO	MgO	SiO_2	V_2O_4	Total	Cations per 6 oxygens VI	IV	Mole fraction $CaMgSi_2O_6$
925	XTL2**	Oen <	28	0.64	38.96	59.06	0.30	98.97	1.988	2.006	0.023(1)
		Dio >	26	23.53	20.64	55.64	0.32	100.13	2.002	1.999	0.901(2)
975	XTL1**	Oen >	21	0.70	39.16	59.29	0.23	99.39	1.992	2.004	0.025(1)
		Dio <	11	23.02	20.93	55.91	0.30	100.17	1.994	2.003	0.883(2)
	XTL2**	Oen <	14	0.79	39.03	59.45	0.23	99.50	1.986	2.007	0.028(1)
		Dio >	25	22.90	20.93	55.57	0.38	99.78	1.997	2.002	0.881(2)
975	XTL9	Oen + Dio + For‡									
985	XTL9	Oen + Dio + For‡									
995	XTL9	Oen + Dio + For‡									
1005	XTL9	Pen + Oen + Dio + For‡									
1015	XTL9	Pen + Dio + For‡									
1025	XTL9	Pen + Dio + For‡									
1025	XTL1**	Pen >	13	0.64	39.35	59.47	0.29	99.75	1.992	2.004	0.023(1)
		Dio <	12	22.48	21.44	55.67	0.72	100.30	1.996	2.002	0.860(2)
	XTL2**	Pen <	28	0.68	39.30	59.13	0.25	99.36	2.000	2.000	0.025(1)
		Dio >	39	22.22	21.82	55.81	0.34	100.19	2.006	1.997	0.845(2)
1075	XTL1**	Pen >	13	0.66	39.46	59.81	0.26	100.18	1.989	2.005	0.024(1)
		Dio <	16	21.85	21.66	55.88	0.57	99.96	1.986	2.007	0.841(3)
	XTL2**	Pen <	14	0.68	38.99	58.84	0.21	98.72	1.997	2.002	0.025(1)
		Dio >	18	21.99	21.85	55.64	0.37	99.84	2.005	1.997	0.840(2)
1125	XTL1**	Pen >	14	0.73	39.11	59.25	0.19	99.27	1.993	2.004	0.026(1)
		Dio <	14	21.74	21.94	55.60	0.57	99.85	1.999	2.000	0.832(2)
	XTL2**	Pen <	13	0.73	39.22	59.64	0.39	99.70	1.989	2.006	0.026(1)
		Dio >	16	21.79	22.08	55.83	0.40	100.09	2.003	1.999	0.830(2)
1175	XTL1**	Pen >	30	0.76	39.22	59.38	0.15	99.52	1.995	2.003	0.028(1)
		Dio <	23	21.21	22.70	55.92	0.47	100.30	2.007	1.997	0.804(2)
	XTL3	Pen <	20	0.89	39.30	59.45	0.41	100.05	1.995	2.002	0.032(1)
		Dio >	23	21.01	22.74	55.94	0.63	100.33	2.000	2.000	0.798(2)
1225	XTL1	Pen >	9	0.91	39.12	59.76	0.30	100.09	1.984	2.008	0.033(1)
		Dio <	17	20.43	22.91	56.29	0.54	100.16	1.985	2.008	0.781(4)
	XTL3	Pen <	16	0.89	39.41	59.42	0.38	100.10	2.000	2.000	0.032(1)
		Dio >	10	20.19	23.24	56.34	0.58	100.36	1.989	2.006	0.769(2)
1275	XTL1	Pen >	14	0.98	39.19	59.40	0.19	99.76	1.998	2.001	0.036(1)
		Dio <	16	19.71	23.72	55.94	0.47	99.85	2.005	1.998	0.748(3)
	XTL3	Pen <	13	1.04	39.07	59.52	0.21	99.83	1.992	2.004	0.038(1)
		Dio >	14	19.63	23.63	55.82	0.48	99.56	2.002	1.999	0.748(3)
1285	GLS1	Pen	10	1.03	39.06	60.10	0.17	100.36	1.980	2.010	0.037(2)
		Dio	10	19.42	23.57	55.64	0.46	99.09	1.999	2.001	0.744(3)
1295	XTL3	Pen >	6	0.95	39.34	60.37	0.17	100.82	1.981	2.010	0.034(1)
		Pig	10	4.63	36.58	59.12	0.22	100.55	2.004	1.998	0.167(2)
		Dio <	7	19.49	24.06	56.93	0.37	100.85	1.989	2.005	0.736(5)
	XTL5	Pen	10	1.01	39.06	60.22	0.21	100.50	1.976	2.008	0.036(1)
		Pig <	18	4.74	36.39	59.15	0.28	100.56	1.999	2.001	0.171(2)
		Dio >	15	19.37	23.92	56.69	0.56	100.54	1.984	2.008	0.736(3)
	XTL7	Pen <	6	0.98	39.34	60.27	0.19	100.79	1.984	2.008	0.035(1)
		Pig >	13	4.52	36.69	59.26	0.34	100.82	2.000	2.000	0.163(3)
		Dio	10	19.23	23.32	56.09	0.38	99.02	1.985	2.008	0.735(2)
1305	GLS1	Pig	18	4.60	36.52	59.15	0.25	100.52	2.001	2.000	0.166(2)
		Dio	9	19.28	24.07	56.77	0.37	100.49	1.988	2.006	0.731(3)
1325	XTL4	Pig >	29	5.02	35.95	59.69	0.17	100.82	1.981	2.010	0.183(1)
		Dio <	26	19.29	24.26	57.05	0.43	101.03	1.987	2.006	0.728(2)
	XTL5	Pig <	33	5.14	35.86	59.30	0.18	100.48	1.989	2.005	0.187(2)
		Dio >	32	18.75	24.76	56.76	0.32	100.58	2.000	2.000	0.705(3)
1350	XTL4	Pig >	15	5.43	35.46	58.91	0.16	99.96	1.992	2.004	0.198(1)
		Dio <	13	18.35	24.83	56.56	0.28	100.02	1.998	2.001	0.694(1)
	XTL5	Pig <	15	5.50	35.60	59.01	0.15	100.26	1.996	2.002	0.200(1)
		Dio >	16	18.28	25.29	56.72	0.28	100.57	2.008	1.996	0.684(3)
1375	XTL4	Pig >	20	5.77	34.98	58.83	0.09	99.67	1.987	2.007	0.212(2)
		Dio <	11	17.97	25.25	56.39	0.19	99.80	2.008	1.996	0.677(3)
1305	GLS2	Pen	7	0.96	39.17	59.80	0.20	100.12	1.988	2.006	0.035(1)
		Pig	21	4.33	36.76	59.25	0.25	100.60	2.000	2.000	0.156(1)
1325	XTL6	Pen >	6	0.86	39.30	59.48	0.12	99.76	1.998	2.001	0.031(1)
		Pig <	17	3.96	36.91	59.14	0.19	100.21	1.999	2.000	0.143(1)
	XTL7	Pen <	15	0.93	39.26	59.63	0.14	99.96	1.995	2.003	0.033(1)
		Pig >	10	3.87	37.14	59.03	0.22	100.26	2.007	1.997	0.139(2)

TABLE 2—*Continued*

T (°C)	Reactant*	Products†	*n*	Weight percent					Cations per 6 oxygens		Mole fraction $CaMgSi_2O_6$
				CaO	MgO	SiO_2	V_2O_4	Total	VI	IV	
1350	XTL6	Pen >	6	0.83	39.55	59.78	0.10	100.26	2.000	2.000	0.030(1)
		Pig <	23	3.61	37.55	59.32	0.16	100.64	2.009	1.996	0.129(1)
	XTL7	Pen <	11	0.93	39.32	59.81	0.11	100.17	1.993	2.003	0.034(1)
		Pig >	10	3.34	37.49	59.43	0.16	100.41	1.998	2.001	0.120(1)
1360	GLS2	Pen	10	0.83	39.53	59.77	0.08	100.29	2.001	1.999	0.033(1)
		Pig	10	3.15	37.32	59.51	0.12	100.10	1.986	2.007	0.114(1)
1370	GLS2	Pen	7	0.91	39.12	59.96	0.08	100.07	1.984	2.008	0.033(1)
		Opx	7	2.14	38.37	60.02	0.10	100.63	1.986	2.007	0.077(1)
		Pig	20	3.08	37.50	59.56	0.11	100.25	1.990	2.005	0.112(1)
1380	OXD6	Opx	29	2.06	38.30	59.56	0.06	99.99	1.993	2.004	0.075(1)
		Pig	23	2.90	37.70	59.59	0.10	100.30	1.992	2.004	0.105(1)
1400	OXD6	Opx	15	1.95	38.18	59.27	0.03	99.43	1.993	2.004	0.071(1)
		Pig	13	2.69	37.51	59.03	0.04	99.28	1.994	2.003	0.098(1)
1380	OXD7	Pen	25	0.82	39.31	60.04	0.14	100.31	1.985	2.008	0.030(1)
		Opx	26	1.90	38.42	60.01	0.14	100.47	1.982	2.009	0.069(1)
1400	OXD7	Pen	10	0.77	39.18	59.58	0.07	99.59	1.990	2.005	0.028(1)
		Opx	7	1.81	38.44	59.44	0.07	99.76	1.994	2.003	0.065(1)
1425	OXD7	Pen	14	0.69	39.95	59.89	0.05	100.58	2.008	1.996	0.024(1)
		Opx	8	1.49	39.20	59.81	0.06	100.57	2.004	1.998	0.053(1)

Note: Abbreviations: *n* = number of crystals analyzed; VI = Ca + Mg; IV = Si + V; numbers in parentheses represent the standard error of the mean for least-significant figure.

* All runs also included saturated solvents with compositions as given in Fig. 2. Runs marked with double asterisks (**) contained, in addition, 10% by weight of XTL9 as seeds (cf. Carlson, 1986b).

† Runs that represent compositional reversals are indicated as follows: >, composition approached from lower mole fraction $CaMgSi_2O_6$; <, composition approached from higher mole fraction $CaMgSi_2O_6$.

‡ From X-ray powder diffraction; no chemical analysis.

both Table 2 and Figure 3 incorporate some data presented earlier (Carlson, 1985, 1986b), which have been supplemented by additional experiments and analyses as described below.

Oen + Dio equilibria and the reaction Oen = Pen + Dio

The recognition of the [Pig] equilibrium at atmospheric pressure is critical to discrimination among the four proposed alternative interpretations of the phase relations. For this reason, the reversal of this equilibrium at 1005 ± 10 °C published by Carlson (1985) has been re-examined. In order to eliminate, insofar as possible, any effects arising from the use of the vanadate solvent in the earlier determination, the equilibrium was redetermined in experiments using PbO as an alternative solvent. Because of the large difference in ionic radii between Pb and V, their effects on the equilibria should be largely opposite in nature, and this contrast should have accentuated any small influences that either solvent had upon the pyroxene equilibria.

The results suggest that neither solvent appreciably displaces the equilibrium. Runs at 10 °C intervals from 975 °C to 1025 °C using the plumbate solvent replicated precisely the results of the earlier study using vanadate solvents: the starting material consisting of Pen/Cen + Oen + Dio + For (forsterite) recrystallized to Pen/Cen + Dio + For at temperatures above 1005 °C, but recrystallized to Oen + Dio + For at temperatures below 1005 °C, and retained the four-phase assemblage in the run at 1005 °C.

Pen + Dio equilibria and the reaction Pen + Dio = Pig

Previously published data on coexisting Pen + Dio in the range 1025–1175 °C (Carlson, 1986b) have been augmented by additional compositional reversals from 1175 °C to 1275 °C, and a synthesis result at 1285 °C.

Syntheses from glass starting materials produced Pen/Cen + Dio + For at 1285 °C, Pen/Cen + Pig + Dio + For at 1295 °C, and either Pen/Cen + Pig + For or Pig + Dio + For at 1305 °C. The equilibrium thus implied at 1295 ± 10 °C was reversed in terms of the compositions of coexisting phases by the runs listed at 1295 °C in Table 2, in which each of the two-pyroxene equilibria possible at higher and lower temperatures was re-equilibrated to 1295 °C. In all cases, a three-pyroxene assemblage was produced that lacked any textural evidence of disequilibrium, as illustrated by the example of textural relations in Figure 4. The analyzed compositions in these reversals produce brackets in good agreement with the miscibility gaps at higher and lower temperatures shown in Figure 3.

Pig + Dio equilibria

Assemblages of Pig + Dio + For, synthesized from glass at 1305 °C and at 1375 °C, were re-equilibrated to higher and lower temperatures, respectively. The results

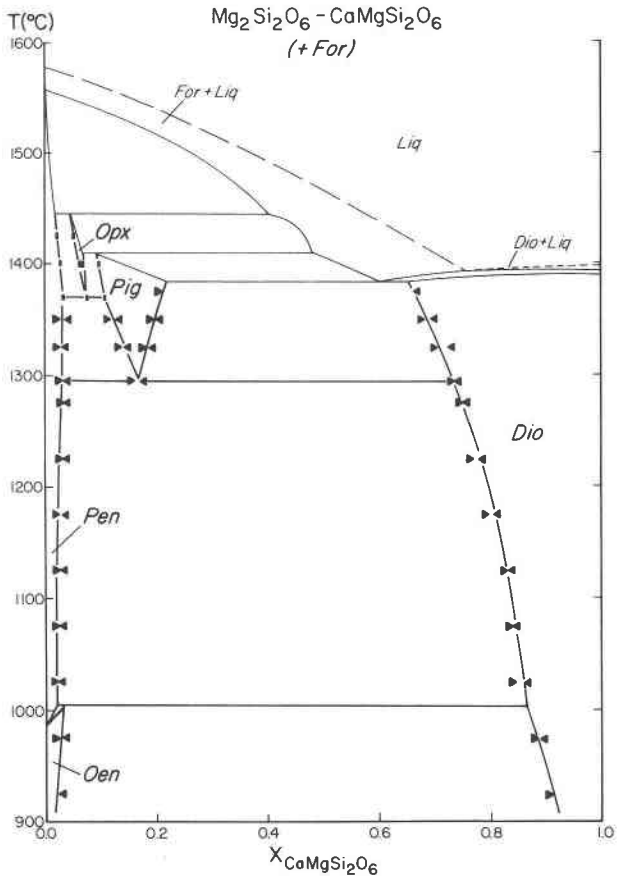

Fig. 3. Phase relations on the forsterite-saturated join $Mg_2Si_2O_6$-$CaMgSi_2O_6$ at atmospheric pressure. Supersolidus equilibria are from Longhi and Boudreau (1980). Compositional reversals are shown by arrowheads indicating the direction of approach to equilibrium, with arrowpoints located at analyzed mean compositions. Each synthesis result is indicated by a rectangle, the width of which is twice the standard error of the mean of analyzed compositions in the run.

provide two-sided limits on the compositions of coexisting Pig + Dio at 1325 °C and at 1350 °C, and a half-bracket constraining the maximum width of the miscibility gap at 1375 °C.

Pen + Pig equilibria and the reaction Pen + Pig = Opx

The determination of the compositions of coexisting Pen + Pig in the temperature range 1295–1370 °C was not straightforward. Although both Pen/Cen and Pig were present in all runs of appropriate bulk composition in the temperature range 1295–1370 °C, complications arose from the highly capricious appearance of Opx in some runs. None of the synthesis runs using glass reactants ever produced Opx. About one-third of the attempted compositional reversals that employed a crystalline mixture of Pen/Cen + Pig + For as starting material were found to contain small but variable amounts of Opx in addition to Pen/Cen + Pig; the remaining two-thirds did not have detectable amounts of Opx. Additional syntheses using oxides as starting materials likewise produced Opx in

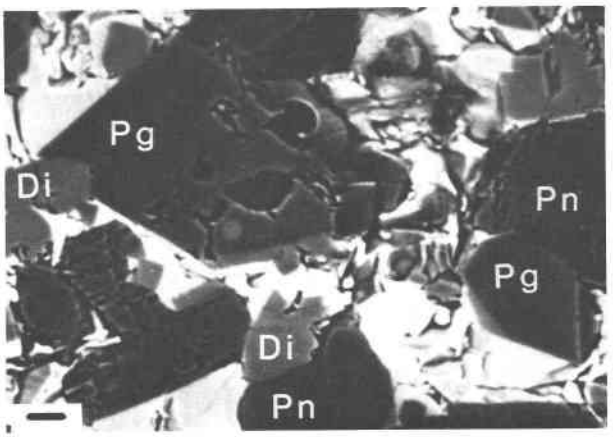

Fig. 4. Backscattered-electron image of textural relations on a polished section through a run displaying the isobaric invariant assemblage Pen + Pig + Dio + For + solvent-rich melt at 1295 °C. Scale bar at lower left is 10 μm in length.

roughly one-third to one-half of the runs. Despite the fact that re-running the Opx-bearing charges for durations up to 10 d failed to eliminate the Opx, the phase is judged to be metastable, for reasons elaborated in the section below concerning stability limits for Opx. The data appearing in Table 2 were obtained exclusively from Opx-free runs in which crystalline mixtures of Pen/Cen + Pig + For, synthesized from glass at 1305 °C and 1360 °C, were re-equilibrated to 1325 °C and 1350 °C.

Synthesis runs from glass reactants produced Pen/Cen + Pig + For at 1360 °C, Pen/Cen + Opx + Pig + For at 1370 °C, and either Pen/Cen + Opx + For or Opx + Pig + For at 1380 °C. Nevertheless, a convincing reversal of the implied equilibrium at 1370 °C was not possible. Although crystalline mixtures of Pen/Cen + Pig + For react completely at temperatures above 1370 °C to yield either of the two Opx-bearing assemblages, all attempts to re-equilibrate the two Opx-bearing assemblages to temperatures below 1370 °C produced the assemblage Pen/Cen + Pig + Opx + For, suggesting metastable persistence of Opx to low temperatures outside of its stability field. Figure 5 illustrates textural relations in a synthesis run at 1370 °C.

Opx + Pig equilibria and Pen + Opx equilibria

Syntheses from oxide mixes produce Opx + Pig + For at 1380 and 1400 °C as well as Pen/Cen + Opx + For at 1380, 1400, and 1425 °C. No attempt was made to obtain compositional reversals of these equilibria, because of the narrow range of compositional variation accessible along these miscibility gaps and because of the controls provided by the supersolidus equilibria and by previous experimentation at these high temperatures.

Discussion

Comparison of results with previous data

Because of the extremely slow reaction kinetics in this system at low subsolidus temperatures, many of the un-

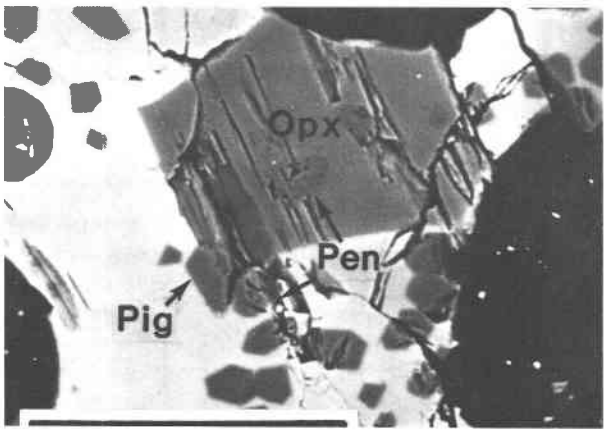

Fig. 5. Backscattered-electron image of textural relations on a polished section through a synthesis run displaying the isobaric invariant assemblage Pen + Opx + Pig + For + solvent-rich melt at 1370 °C. Black ovals are epoxy-filled vesicles. Scale bar at lower left is 100 μm in length.

reversed data from prior experimentation at temperatures below ~1300 °C are unreliable. For the same reason, care must be exercised in evaluating even the existing higher-temperature data; indications of incomplete equilibration and inaccuracies of phase identification and analysis can be expected in this exceedingly recalcitrant system.

Biggar (1985) has provided an excellent comprehensive review of the data available from numerous earlier studies, but the resulting compilation of subsolidus data displays considerable scatter, making precise delineation of stability fields and miscibility gaps impossible. Against the backdrop of the phase diagram presented here in Figure 3, however, a recognizable subset of the earlier data is seen to be in excellent agreement. A detailed comparison of the present results with other published data is made in Figure 6. Analyses from other sources appearing in Figure 6 were selected for inclusion by application of the following criteria: (1) only compositions obtained by microprobe analysis are included; (2) all silica-saturated (tridymite-bearing) experiments are excluded; and (3) experiments displaying a wide range of compositions for a single phase are excluded. The first criterion eliminates the inherently large errors that arise from assigning compositions based on X-ray determinative curves. The second criterion takes into account the possibility of variation in Ca/Mg ratio between forsterite-saturated and tridymite-saturated pigeonite (cf. Biggar, 1985, p. 49), and by extension, that possibility for the other pyroxenes stable in this portion of the phase diagram. Results for tridymite-saturated runs also display greater internal inconsistencies than comparable data sets at forsterite saturation. This may reflect unfavorable kinetic factors that impede the achievement of equilibrium in tridymite-saturated runs. The third criterion eliminates those experiments in which the achievement of equilibrium is least certain.

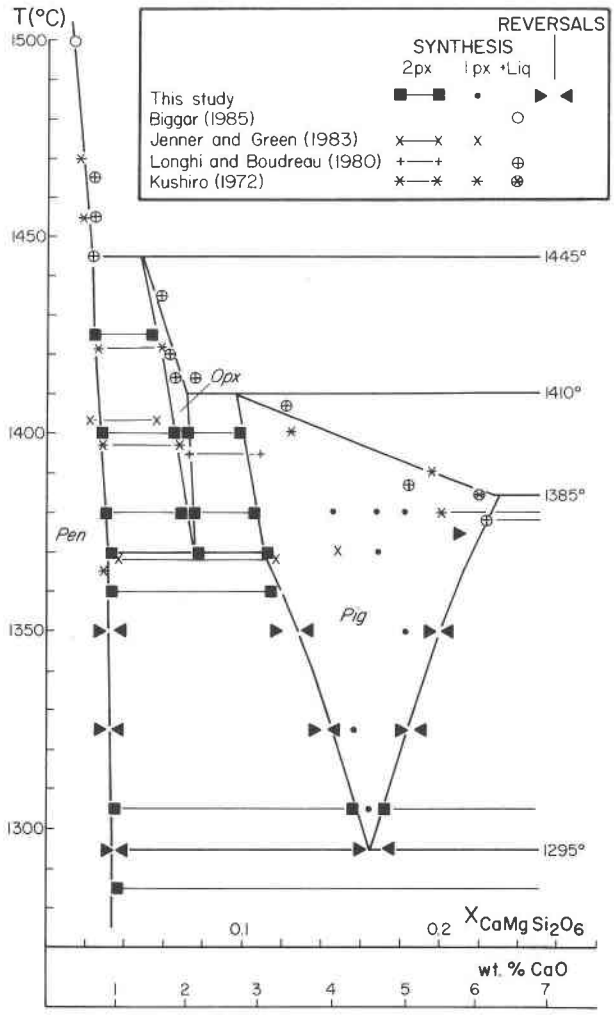

Fig. 6. Comparison of results of present study with selected data from previous investigations in the Mg-rich portion of the diagram at high temperatures. Selection criteria described in text. Coexisting pyroxenes are connected by light lines; pyroxenes in equilibrium with silicate melt are circled.

The subset of earlier data selected on the basis of these criteria is shown by Figure 6 to be in excellent agreement with the phase equilibria determined in the present study. Apart from some scatter in the data constraining the temperature of the Pig + Dio + For + Liq equilibrium and the composition of Pig along the neighboring solidus, the only remaining discrepancy of importance is the matter of phase identification in the 1370 °C run of Jenner and Green (1983). Those authors (their Table I, p. 157) identify the two pyroxenes in that run as Opx + Pig, while acknowledging substantial difficulties and considerable uncertainties in phase recognition in their fine-grained run products. An examination of the data presented in Figure 6, and application of Biggar's (1985) criteria for phase identification, leaves little doubt that the actual assemblage present in that run must be Pen + Pig, as Biggar (1985, p. 57) correctly inferred.

Effects of solvents on phase equilibria

Three features of these experiments lead to the conclusion that incorporation of small amounts of solvent components into the pyroxenes has a negligible effect on the pyroxene phase equilibria. Most significant is the agreement demonstrated above between the results of high-temperature conventional experiments and those of the experiments employing a vanadate solvent. The additional demonstration that two different solvents yield identical results for the location of the [Pig] reaction, despite the expectation of opposite crystal-chemical interactions with the pyroxenes, indicates that effects of solvent contamination remain negligible at temperatures as low as 1000 °C. Finally, the data in Table 2 show a strong decrease in V_2O_4 incorporation in each pyroxene with increasing temperature above ~1200 °C. This decrease is consistent with the petrographic observation (Carlson, 1986b, p. 222) that much of the V in low-temperature pyroxenes may reside in microscopic inclusions of quenched solvent-rich melt, which are numerous only in low-temperature run products; if instead the V were present wholly in solid solution in the pyroxenes, the tendency would probably be toward increasing incorporation of V as temperatures rise. Thus the analyzed V_2O_4 contents are viewed as maximum limits on the amounts of V actually in solid solution, and they probably overestimate, especially at low temperatures, the actual extent of solvent contamination.

Stability limits for Opx

The scattered and inconstant appearance of Opx in runs at temperatures from 1295 to 1370 °C creates ambiguity in that portion of the phase diagram displaying the greatest complexity. I have interpreted this phase to be present metastably over this temperature range for the following reasons.

First, Opx in this temperature range appears unpredictably, being present in some but by no means all runs; it is always found together with Pen + Pig in an assemblage that is highly unlikely to be at equilibrium over a range of temperatures, considering that it consists of five phases (Opx, Pen, Pig, For, and Liq) in a four-component system (CaO, MgO, SiO_2, and V_2O_5). Its appearance is restricted to runs using either crystalline or oxide starting materials; it was not observed in synthesis runs from glass. This situation strongly suggests that Opx may be inherited from chance nucleation in some of the starting mixes. The phase is found only in runs in which Pig is stable instead of Dio and was never produced within the stability field shown for Pen + Dio (below 1295 °C); this again indicates that certain precursor materials may be present that cause metastable crystallization in this temperature range.

Second, the compositions of Opx in equilibrium with Pen, and of Opx in equilibrium with Pig, converge to the same value as temperature drops toward 1370 °C, indicating that the Opx stability field must pinch out there. The compositions of Opx found in disequilibrium assemblages at lower temperatures are excessively calcic when compared to that of Opx in simultaneous equilibrium with both Pig and Pen at 1370 °C; those presumably metastable compositions increase steadily in calcia from about 2 wt% CaO at 1370 °C to just above 3 wt% CaO at 1295 °C.

Third, the data available from other sources in this range of temperature and composition support the stability of Pen + Pig rather than of Opx. Longhi and Boudreau (1980) and Biggar (1985) present reinterpretations of earlier data from Boyd and Schairer (1964), Schwab and Jablonski (1973), Kushiro (1972), and Foster and Lin (1975). Although these reinterpretations require retrospective identification of Opx in runs made before the existence of the phase was recognized, all of them are consistent with a lower limit for Opx stability very near 1370 °C. Two syntheses of the assemblage Pen + Pig are recorded: one is at 1305 °C, 1 atm, from Warner and Luth (1974); the other is at 1370 °C, 1 atm, in the above-mentioned run of Jenner and Green (1983) in which Pen was probably misidentified as Opx.

As reported above, attempts to demonstrate definitively the metastability of Opx below 1370 °C by increasing run durations and by unloading, regrinding, and rerunning charges were unsuccessful; Opx persisted in these runs without evidence of any change of abundance and without any textural indication of resorption. This difficulty makes it prudent, despite the reasons just discussed, to retain as an alternate hypothesis the possibility that Opx may be stable to temperatures lower than the 1370 °C preferred here as the most probable limit.

Asymmetry in the clinopyroxene solid solution

Most thermodynamic models of phase equilibria in this system treat Pig and Dio at high temperature as parts of a single *C*2/*c* clinopyroxene solid solution, with marked positive nonideality accounting for separation into two compositionally distinct phases. Formerly, the only reversed determination of the compositions of coexisting Pig and Dio was that of Schweitzer (1982) at 15 kbar and 1465 °C. That experiment presents an interesting ambiguity: although the midpoints of the two brackets are not symmetric about the compositional midline, the width of the brackets is sufficient to include symmetric compositions as well. The two most recent thermodynamic models in this system differ principally in their approach to this ambiguity, insofar as Lindsley et al. (1981) preferred an asymmetric formulation, whereas Nickel and Brey (1984) argued that the clinopyroxene solution may be treated as symmetric. The data in this study on coexisting Pig and Dio clearly indicate asymmetry at atmospheric pressure, which probably accounts in large part for the relative success at low pressures of the earlier model in comparison to the latter.

Implications and conclusions

Among published studies, only this set of experiments covers the entire range of temperatures required to define

the relations among all currently known pyroxenes in this system. The acquisition of reversed data at low subsolidus temperatures (some 400–450 °C below the limit for which the achievement of equilibrium could be demonstrated in prior work) allows a meaningful evaluation of the discrepancies among the previously proposed interpretations of the phase equilibria; in particular by confirming the presence on the 1-atm isobar of both [Pig] and [Oen], these data demonstrate that either of the two interpretations advanced by Longhi and Boudreau (1980) and by Carlson (1985, 1986b) is preferred over those of both Jenner and Green (1983) and Biggar (1985).

In comparison to earlier work, this study also offers a considerable increase in the precision of both the compositional and thermal limits on the stability of the pyroxene assemblages. This improvement is principally the consequence of the more rapid reaction kinetics induced by the high-temperature solvent technique. The success of this technique in replicating conventional experimental results at high temperatures, while extending the range of feasible experimentation to far lower temperatures, strongly suggests its use in similar attempts to achieve equilibrium in other recalcitrant systems. The narrow compositional brackets provided by reversals over a large portion of the subsolidus region will allow, for the first time, the incorporation of low-pressure phase-equilibrium constraints into thermochemical models of pyroxene solid solutions in this system (e.g., Carlson and Lindsley, 1986, 1988).

The major question left unanswered in this study is that required to discriminate between the interpretations of Longhi and Boudreau (1980) and of Carlson (1985, 1986b): what is the identity of the orthopyroxene-like phase (Opx) encountered near 1400 °C in this system? The present work defines narrow limits on its range of composition and its thermal stability (despite the apparent tendency for this phase to persist metastably under certain conditions), but the data are still insufficient to conclude that it is distinct from, or equivalent to, Oen. Thus the question reduces to evaluating the plausibility of changes in the thermodynamic properties of the phases, sufficient over a narrow temperature range to impose enough curvature on the solid-solid [Dio] reaction to cause it to intersect the 1-atm isobar after departing the invariant point with slope steeper than that of the [Pig] reaction. Attention should therefore be focused upon careful determination of the structure and properties of Opx, in combination with attempts to locate the invariant point and to determine the P-T trajectories of the univariant equilibria that extend from it.

Acknowledgments

Support for this work was provided by NSF grants EAR-8205867 and EAR-8603755 to the author, by the University of Texas Research Institute, and by the Geology Foundation of the University of Texas at Austin. I am grateful to J. Longhi, D. H. Lindsley, and G. M. Biggar for numerous helpful discussions and exchanges. Thoughtful reviews by S. A. Morse and P. M. Davidson are appreciated.

References cited

Atlas, Leon. (1952) The polymorphism of $MgSiO_3$ and solid-state equilibria in the system $MgSiO_3$-$CaMgSi_2O_6$. Journal of Geology, 60, 125–147.

Biggar, G.M. (1985) Calcium-poor pyroxenes: Phase relations in the system CaO-MgO-Al_2O_3-SiO_2. Mineralogical Magazine, 49, 49–58.

Boyd, F.R., and Schairer, J.F. (1964) The system $MgSiO_3$-$CaMgSi_2O_6$. Journal of Petrology, 5, 275–309.

Carlson, W.D. (1985) Evidence against the stability of orthoenstatite above ~1005 °C at atmospheric pressure in CaO-MgO-SiO_2. Geophysical Research Letters, 12, 409–411.

——— (1986a) Vanadium pentoxide as a high-temperature solvent for phase equilibrium studies in CaO-MgO-Al_2O_3-SiO_2. Contributions to Mineralogy and Petrology, 92, 89–92.

——— (1986b) Reversed pyroxene phase equilibria in CaO-MgO-SiO_2 at one atmosphere pressure. Contributions to Mineralogy and Petrology, 92, 218–224.

Carlson, W.D., and Lindsley, D.H. (1986) A thermochemical model for proto-, ortho- and clinopyroxene in the system CaO-MgO-SiO_2. Geological Society of America Abstracts with Programs, 18, 558.

——— (1988) Thermochemistry of pyroxenes on the join $Mg_2Si_2O_6$-$CaMgSi_2O_6$. American Mineralogist, 73, 242–252.

Foster, W.R., and Lin, H.C. (1975) New data on the forsterite-diopside-silica system. EOS, 56, 470.

Jenner, G.A., and Green, D.H. (1983) Equilibria in the Mg-rich part of the pyroxene quadrilateral. Mineralogical Magazine, 47, 153–160.

Kushiro, Ikuo. (1972) Determination of liquidus relations in synthetic silicate systems with electron probe analysis: The system forsterite-diopside-silica at 1 atmosphere. American Mineralogist, 57, 1260–1271.

Lindsley, D.H., Grover, J.E., and Davidson, P.M. (1981) The thermodynamics of the $Mg_2Si_2O_6$-$CaMgSi_2O_6$ join: A review and an improved model. In R.C. Newton, A. Navrotsky, and B.J. Wood, Eds., Thermodynamics of minerals and melts, p. 149–175. Springer-Verlag, New York.

Longhi, John, and Boudreau, A.E. (1980) The orthoenstatite liquidus field in the system forsterite-diopside-silica at one atmosphere. American Mineralogist, 65, 563–573.

Nickel, K.G., and Brey, Gerhard. (1984) Subsolidus orthopyroxene-clinopyroxene systematics in the system CaO-MgO-SiO_2 to 60 kbar: A re-evaluation of the regular solution model. Contributions to Mineralogy and Petrology, 87, 35–42.

Schwab, R.G., and Jablonski, K.H. (1973) Der Polymorphismus der Pigeonite. Fortschritte Mineralogie, 50, 223–263.

Schweitzer, Elaine. (1982) The reaction pigeonite = $diopside_{ss}$ + $enstatite_{ss}$ at 15 kbars. American Mineralogist, 67, 54–58.

Smith, J.V. (1959) The crystal structure of proto-enstatite, $MgSiO_3$. Acta Crystallographica, 12, 515–519.

Smyth, J.R. (1974) Experimental study on the polymorphism of enstatite. American Mineralogist, 59, 345–352.

Warner, R.D. (1975) New experimental data for the system CaO-MgO-SiO_2-H_2O and a synthesis of inferred phase relations. Geochimica et Cosmochimica Acta, 39, 1413–1421.

Warner, R.D., and Luth, W.L. (1974) The diopside-orthoenstatite two-phase region in the system $CaMgSi_2O_6$-$Mg_2Si_2O_6$. American Mineralogist, 59, 98–109.

Yang, H.-Y. (1973) Crystallization of iron-free pigeonite in the system anorthite-diopside-enstatite-silica at atmospheric pressure. American Journal of Science, 273, 488–497.

Yang, H.-Y., and Foster, W.R. (1972) Stability of iron-free pigeonite at atmospheric pressure. American Mineralogist, 57, 1232–1241.

Manuscript received June 22, 1987
Manuscript accepted November 13, 1987